Synthesis and Characterization of CZT Nanoparticles for Sensor Applications

Darsipati Praveen Kumar[1], P Srinivasa Subbarao[2], Dr. Kalapala Prasad[3], Thaneti Lily Rani[4]
[1] *Student, Jntu Kakinada, Andhra Pradesh*
[2,4] *Assistant professor, Jntu Kakinada, Andhra Pradesh*
[3] *Associate professor and HOD Nano Technology, Jntu Kakinada, Andhra Pradesh*

***Abstract*—The development of earth-abundant and non-toxic semiconductor nanomaterials with tunable structural and optical properties is critical for next-generation sensing applications. In this work, copper–zinc–tin (CZT) nanoparticles were synthesized through a controlled wet-chemical route by systematically varying copper and tin precursor molar concentrations while maintaining constant zinc content. The synthesis strategy enables precise modulation of crystallinity, particle size, and defect density, which are key parameters governing sensor performance. Structural analysis using X-ray diffraction confirmed the formation of polycrystalline CZT nanoparticles with improved phase stability upon optimized precursor ratios, while average crystallite sizes were found to lie in the nanometer regime. Morphological investigation via scanning electron microscopy revealed agglomerated yet uniformly distributed nanoscale particles, indicating favorable surface characteristics for adsorption-driven sensing mechanisms. Elemental analysis verified near-stoichiometric composition, demonstrating effective precursor incorporation during synthesis. Optical characterization using UV–visible spectroscopy showed notable band gap variations as a function of precursor concentration, highlighting tunability in the range relevant for optoelectronic and sensing applications. Raman spectroscopy further confirmed phase formation and structural integrity, minimizing ambiguity from secondary phases. The combined results demonstrate that controlled precursor engineering significantly influences the structural and optical response of CZT nanoparticles. Compared to conventional oxide-based sensing materials, CZT offers the advantages of adjustable band gap, high surface activity, and compositional flexibility. The present study establishes a reproducible synthesis–structure–property relationship for CZT nanomaterials and identifies their strong potential as active layers in chemical and optoelectronic sensor devices. This work provides a foundation for future optimization of CZT-based Nanosensors through compositional tuning and surface functionalization.**

***Index Terms*—CZT nanoparticles, Chemical synthesis, XRD, SEM, UV–Visible spectroscopy, Sensors**

I. INTRODUCTION

The rapid advancement of sensor technologies has intensified the demand for semiconductor nanomaterials with tunable electronic properties, high surface activity, and long-term stability. Conventional metal oxide–based sensing materials such as ZnO, SnO_2, and TiO_2, although widely studied, suffer from intrinsic limitations including wide band gaps, restricted spectral response, and limited compositional flexibility. These constraints motivate the exploration of alternative semiconductor systems capable of offering enhanced sensitivity, band gap tunability, and material sustainability.

Quaternary chalcogenide semiconductors have recently emerged as promising candidates due to their compositional versatility and favorable optoelectronic characteristics. Among them, copper–zinc–tin–based compounds (CZT) have attracted growing interest owing to their earth-abundant, low-toxicity elemental constituents and adaptable crystal chemistry. While CZT materials have been extensively investigated as absorber layers in thin-film photovoltaic applications, their potential for sensor applications remains comparatively underexplored. In particular, the influence of precursor stoichiometry on structural evolution, defect formation, and optical behavior of CZT nanoparticles has not been sufficiently established in the context of sensing performance.

At the nanoscale, material properties are strongly governed by crystallite size, surface morphology, and

defect density, all of which directly affect adsorption–desorption processes critical for sensor operation. Controlled synthesis routes that enable precise tuning of these parameters are therefore essential. Existing reports on CZT synthesis primarily focus on thin films or photovoltaic efficiency optimization, often overlooking systematic precursor concentration effects and their implications for nanoscale sensing functionality. Furthermore, secondary phase formation and compositional deviations remain major challenges in achieving reproducible and phase-stable CZT nanostructures.

In this context, the present work addresses the need for a controlled and reproducible synthesis strategy for CZT nanoparticles tailored toward sensor applications. A wet-chemical synthesis approach is employed, wherein the molar concentrations of copper and tin precursors are systematically varied while maintaining constant zinc content. This compositional engineering enables investigation of structure–property correlations and provides insight into how precursor ratios influence crystallinity, particle size, defect density, and optical band gap.

The synthesized CZT nanoparticles are comprehensively characterized using X-ray diffraction, scanning electron microscopy coupled with elemental analysis, UV–visible spectroscopy, and Raman spectroscopy. These techniques collectively elucidate phase formation, morphological features, compositional integrity, and optical response. The study establishes a direct correlation between precursor stoichiometry and material properties relevant to sensing mechanisms, such as surface activity and band gap modulation.

The key contributions of this work are threefold: (i) development of a simple and scalable chemical synthesis route for CZT nanoparticles with controlled composition, (ii) systematic evaluation of the effect of precursor molar variation on structural and optical properties, and (iii) identification of CZT nanoparticles as promising alternative sensing materials beyond their conventional photovoltaic role. The findings provide a foundational framework for further optimization of CZT-based nanomaterials for chemical and optoelectronic sensor devices.

II. MATERIALS AND REAGENTS

- Cupric chloride dihydrate ($CuCl_2 \cdot 2H_2O$) – Copper precursor
- Zinc chloride ($ZnCl_2$) – Zinc precursor
- Stannous chloride dihydrate ($SnCl_2 \cdot 2H_2O$) – Tin precursor
- Sodium hydroxide (NaOH) – pH adjusting agent
- Acetic acid (CH_3COOH) – Reaction stabilizing agent
- Acetone – Final washing solvent
- Deionized water – Solvent for all preparations

Synthesis of CZT Nanoparticles:

CZT nanoparticles were synthesized using a controlled wet-chemical precipitation route. To investigate the effect of precursor stoichiometry, the concentration of copper and tin precursors was systematically varied while keeping the zinc concentration constant.

Separate aqueous solutions of $CuCl_2 \cdot 2H_2O$, $ZnCl_2$, and $SnCl_2 \cdot 2H_2O$ were prepared using deionized water. The zinc precursor concentration was fixed at 0.04 M for all samples. Copper precursor concentrations were varied as 0.12 M, 0.13 M, 0.14 M, and 0.15 M, while the tin precursor concentrations were adjusted correspondingly to 0.04M, 0.03M, 0.02 M, and 0.01 M to maintain compositional balance.

The prepared precursor solutions were mixed under continuous magnetic stirring at room temperature to achieve homogeneous ion distribution. A small amount of acetic acid was added to stabilize the reaction medium. The pH of the mixed solution was adjusted to approximately 7 by the dropwise addition of NaOH solution, promoting controlled nucleation and growth of CZT particles. The reaction mixture was stirred for 1 h at a constant stirring speed.

The resulting precipitate was collected by centrifugation and washed repeatedly with deionized water to remove unreacted ions and by-products, followed by a final wash with acetone to eliminate residual organic impurities. The washed material was dried and subsequently calcined in a muffle furnace at 500 °C for 2 h to enhance crystallinity and phase formation. The same synthesis protocol was applied to all compositions to ensure experimental consistency.

Structural Characterization
- X-ray Diffraction (XRD)
  - Purpose: Phase identification, crystallinity, crystallite size estimation

Morphological and Elemental Analysis
- Scanning Electron Microscopy (SEM)
  - Purpose: Surface morphology and particle distribution
- Energy Dispersive X-ray Spectroscopy (EDS/EDAX)
  - Purpose: Elemental composition and stoichiometry verification

Optical Characterization
- UV–Visible Spectroscopy (UV–Vis)
  - Purpose: Optical absorption behavior and band gap estimation

Vibrational Analysis
- Raman Spectroscopy
  - Purpose: Phase confirmation and detection of secondary phases

Structural Characterization

The crystalline structure and phase composition of the synthesized CZT nanoparticles were analyzed using X-ray diffraction (XRD) with Cu Kα radiation. Diffraction patterns were recorded over a broad 2θ range. Structural parameters including interplanar spacing, average crystallite size, and dislocation density were calculated from the diffraction data to assess the influence of precursor composition on crystal growth and structural quality.

Morphological and Elemental Analysis

Surface morphology and particle distribution were examined using scanning electron microscopy (SEM). Elemental composition and stoichiometry were evaluated using energy-dispersive X-ray spectroscopy (EDS) attached to the SEM system, confirming the presence and relative distribution of copper, zinc, and tin in the synthesized nanoparticles.

Optical Characterization

Optical absorption properties of the CZT nanoparticles were studied using UV–visible spectroscopy in the relevant wavelength range. The absorption spectra were analyzed to estimate optical band gap values and to evaluate the effect of precursor concentration on the electronic structure of the material.

Raman Spectroscopy

Raman spectroscopy was employed to confirm phase formation and assess the structural integrity of the CZT nanoparticles. Characteristic vibrational modes were analyzed to distinguish CZT from possible secondary phases and to validate crystallographic consistency across different compositions.

Experimental Reproducibility

All synthesis and characterization procedures were conducted under identical experimental conditions for each sample. This ensured reproducibility and enabled direct correlation between precursor stoichiometry and the resulting structural and optical properties relevant to sensor applications.

III. RESULTS

X-RAY DIFFRACTION TECHNIQUE

The crystalline structure and phase formation of the synthesized CZT nanoparticles were investigated using X-ray diffraction. The diffraction patterns corresponding to different precursor compositions confirm the formation of polycrystalline CZT phases. Prominent diffraction peaks observed at characteristic 2θ positions are consistent with reported CZT-related reflections, indicating successful incorporation of Cu, Zn, and Sn within the crystal lattice.

Variation in precursor molar concentration significantly influences peak intensity and broadening. Samples prepared with optimized copper and tin ratios exhibit sharper diffraction peaks, reflecting improved crystallinity and grain growth. The average crystallite size, estimated from peak broadening analysis, lies in the nanometre range for all samples, confirming nanoscale formation. An increase in copper concentration with a corresponding decrease in tin concentration results in moderate crystallite size enhancement, suggesting reduced lattice strain and improved crystal ordering.

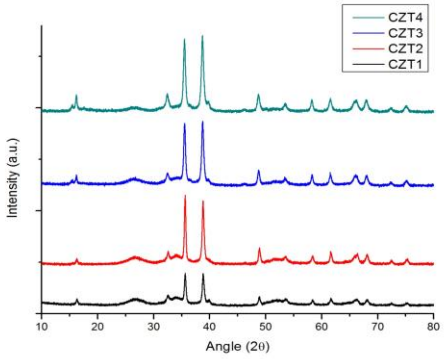

Dislocation density values calculated from crystallite size data show a decreasing trend for samples with improved crystallinity. Lower dislocation density indicates reduced defect concentration, which is beneficial for stable electronic transport and sensing behaviour. These results demonstrate that precursor stoichiometry plays a decisive role in tailoring the structural quality of CZT nanoparticles.

SCANNING ELECTRON MICROSCOPE:

a) SEM image of 0.12M $CuCl_2.2H_20$ AND 0.04M SnCl2

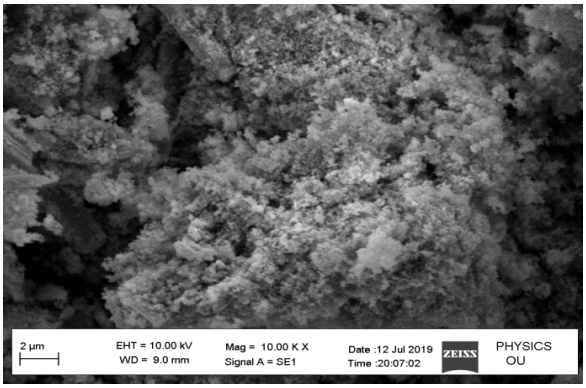

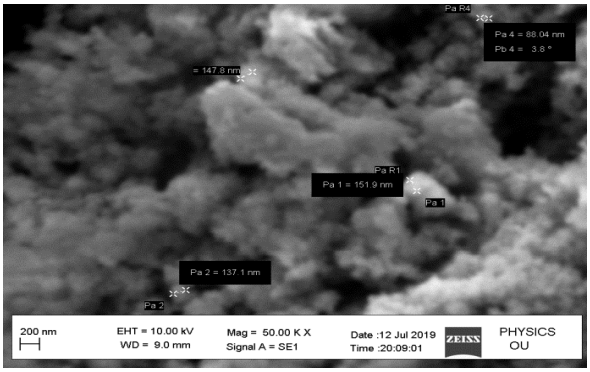

Fig: SEM image of CZT 2µm and 200nm

(b) SEM image of 0.13M $CuCl_2.2H_20$ AND 0.03M $SnCl_2$

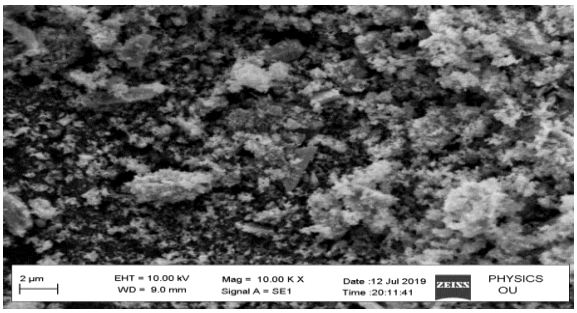

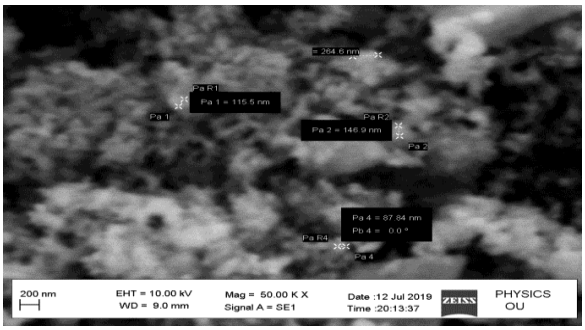

Fig: SEM image of CZT 2µm and 200nm

c) SEM image of 0.14M $CuCl_2.2H_20$ AND 0.02M $SnCl_2$

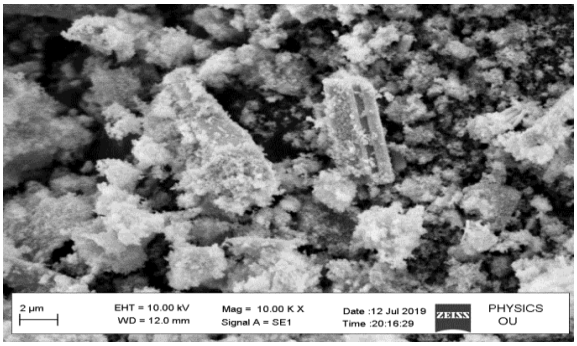

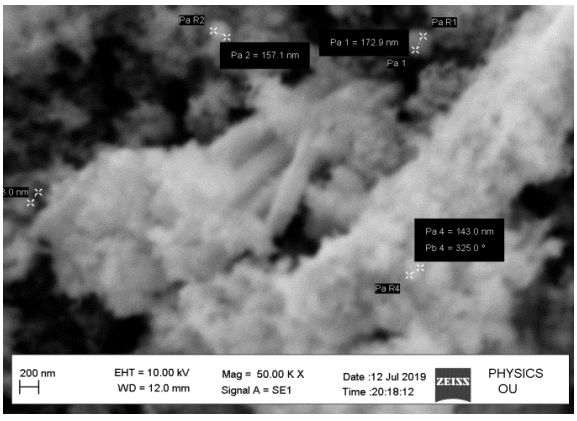

Fig: SEM image of CZT 2µm and 200nm

(d) SEM image of 0.15M $CuCl_2.2H_20$ AND 0.01M SnCl2

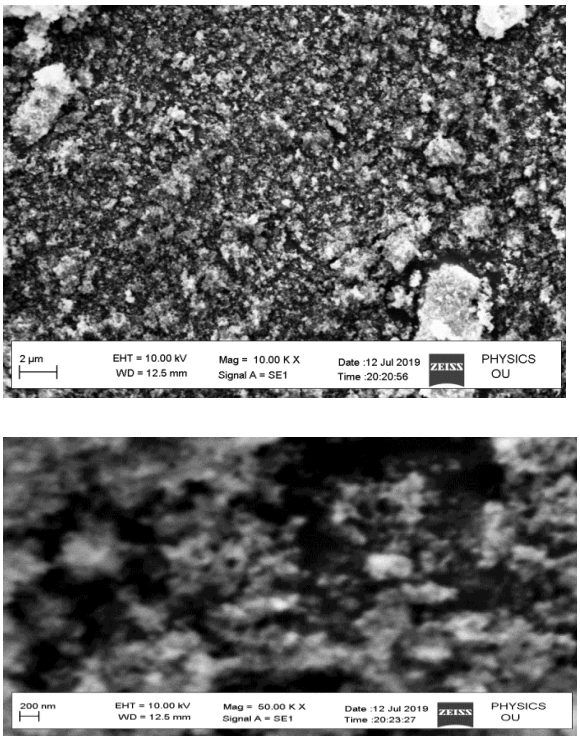

Fig: SEM image of CZT 2µm and 200nm

Energy-dispersive X-ray spectroscopy confirms the presence of copper, zinc, and tin in all synthesized samples. The elemental ratios closely match the intended precursor compositions, indicating effective incorporation of constituent elements during synthesis. No extraneous elemental peaks are detected, confirming minimal contamination and good chemical purity of the samples.

Elemental analysis by EDAX:

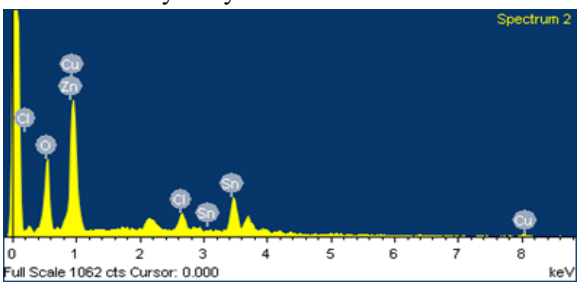

Element	Weight%	Atomic%
O K	22.34	57.60
Cl K	3.86	4.49
Cu L	34.30	22.26
Zn L	6.77	4.27
Sn L	32.72	11.37
Totals	100.00	

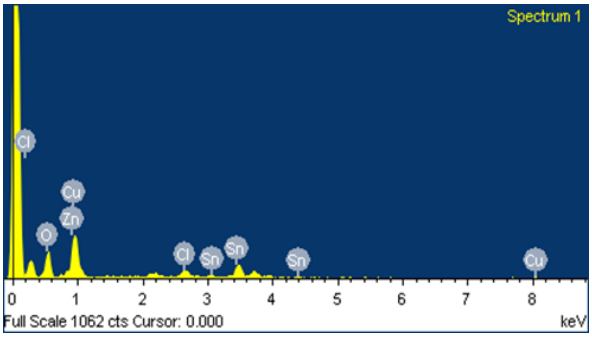

Element	Weight%	Atomic%
O K	21.62	56.25
Cl K	3.74	4.40
Cu L	37.94	24.86
Zn L	5.66	3.60
Sn L	31.04	10.89
Totals	100.00	

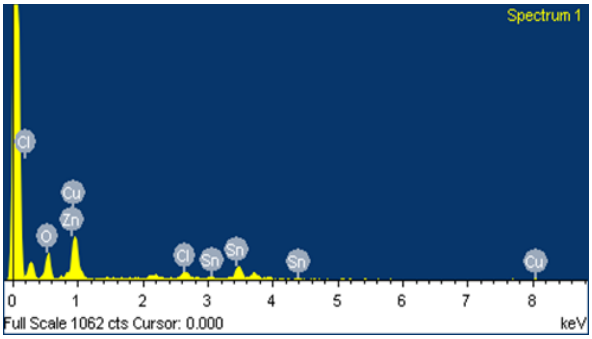

Element	Weight%	Atomic%
O K	20.59	57.60
Cl K	3.47	4.49
Cu L	39.30	22.26
Zn L	5.9	4.14
Sn L	26.50	9.07
Totals	100.00	

The combined SEM and EDS results demonstrate that the wet-chemical synthesis route enables reproducible formation of CZT nanoparticles with controlled composition and favorable surface characteristics.

IV. UV-VISIBLE SPECTROSCOPY

The optical properties of CZT nanoparticles were

examined using UV–visible spectroscopy. All samples exhibit strong absorption in the visible region, which is essential for optoelectronic and sensor-related applications. A clear shift in the absorption edge is observed with variation in precursor composition, indicating tunability of the optical band gap.

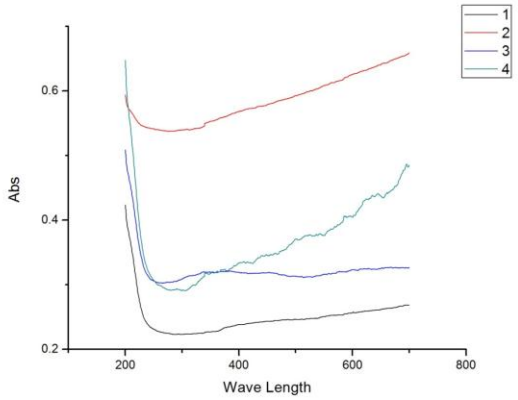

Fig: spectroscopy graph

Estimated band gap values show systematic variation as the copper concentration increases and tin concentration decreases. This behavior can be attributed to changes in crystallite size, defect density, and electronic structure induced by precursor stoichiometry. Samples with smaller crystallite size and higher defect concentration exhibit relatively larger band gap values, consistent with quantum confinement and disorder effects at the nanoscale.

Band-gap graphs:

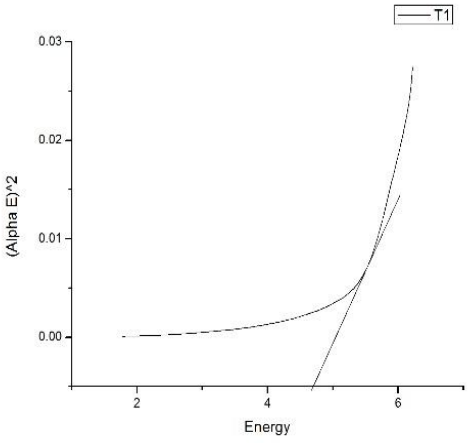

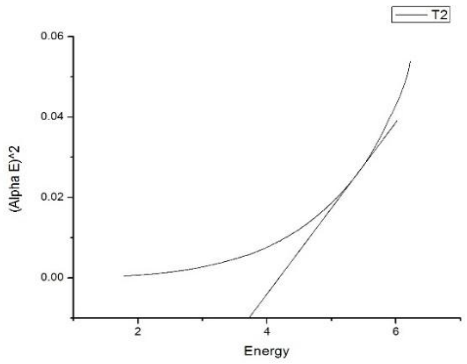

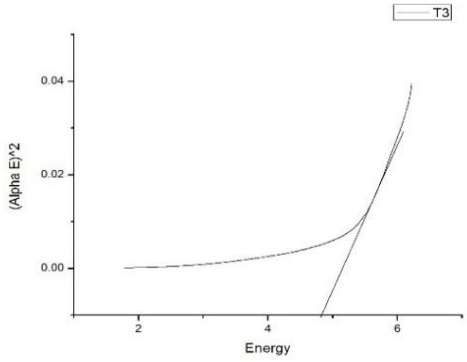

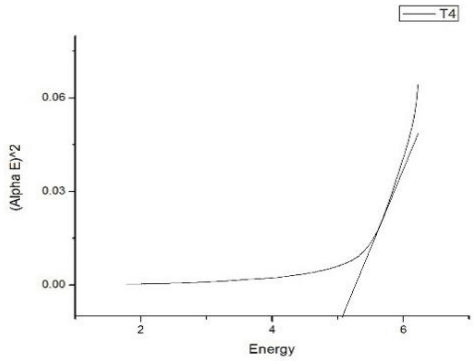

The ability to tune the band gap through simple precursor control provides a significant advantage over conventional binary metal oxide sensing materials, enabling flexibility in sensor response and operating conditions.

V. RAMAN SPECTROSCOPY

Raman spectroscopy was employed to further validate phase formation and structural integrity of the CZT nanoparticles. The recorded Raman spectra show characteristic vibrational modes associated with

CZT, confirming the formation of the desired phase. The absence of strong secondary-phase peaks suggests minimal formation of unwanted sulfide or oxide phases. Raman spectroscope gives the graph between intensity and Raman shift. Raman spectroscopy measurements were done on the CZT prepared by Sol-Gel method. The fitting with Lorentzian functions curves of the Raman spectrum of the evaporated sample gives evidence of peaks presence at 262, 287, 302, 338, 367 and 374cm-1 which have been attributed to the CZT.

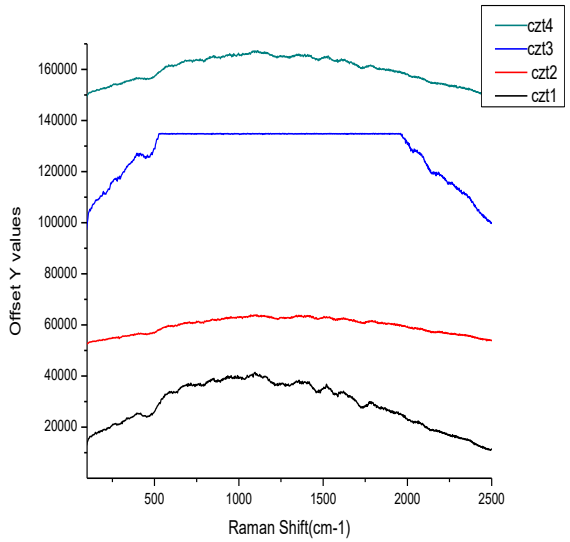

Fig. Raman Spectra of Sample

According to the figure 7.4 When we doped the Nickel into pure zine oxide nano particulars that Raman peak are gradually changed with respectively concentration such as Pure, 0.01%, 0.02%, 0.03%, 0.04% of molar Nickel doped ZnO, with their characteristic's bands corresponding to 595cm^{-1}. The above Raman peak gradually decreases and the peak 620cm^{-1} is gradually increases due to the Nickel doping into host lattice. So related to intrinsic host lattice defects which is become a spectroscopically vibrational active.

Subtle variations in peak width and intensity across different samples reflect changes in crystallinity and lattice disorder, which correlate well with XRD observations. Raman analysis thus supports the conclusion that precursor molar variation directly influences structural ordering at the atomic scale.

Correlation Between Structure, Optical Properties, and Sensor Relevance

By correlating structural, morphological, and optical results, a clear structure–property relationship is established. CZT nanoparticles synthesized with optimized precursor ratios exhibit improved crystallinity, reduced defect density, tuneable band gap, and nanoscale morphology with high surface activity. These characteristics are highly desirable for sensor applications, where surface adsorption and charge transfer processes dominate performance.

Unlike conventional metal oxide sensors that often require doping to achieve band gap modulation, CZT offers intrinsic compositional flexibility using earth-abundant and non-toxic elements. The results confirm that CZT nanoparticles possess significant potential as alternative sensing materials, extending their applicability beyond photovoltaic absorber layers.

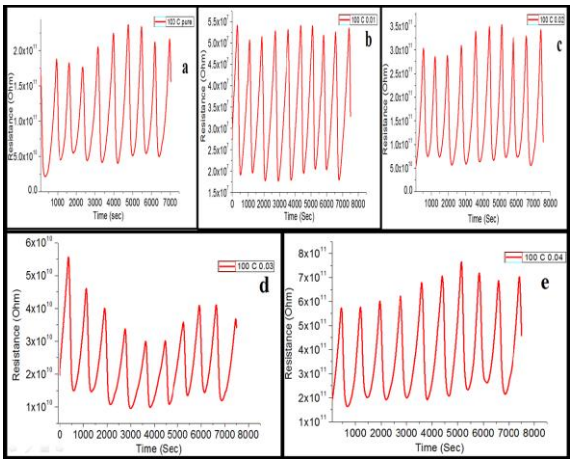

FIG Resistance Vs Time graph

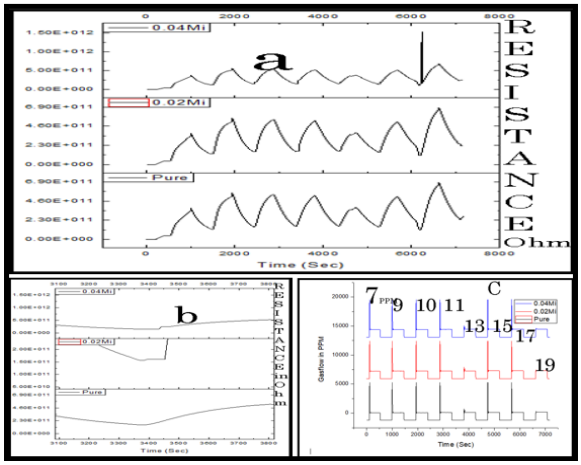

FIG. Shows the a) Resistance Vs Time graph b) saturation point and c) Flow of gas

VI. CONCLUSION

Synthesis Approach

- CZT nanomaterials were successfully synthesized using a low-cost sol–gel method, demonstrating a simple and scalable preparation route.

Precursor Concentration Optimization

- Copper and tin precursor concentrations were varied as 0.12 M–0.15 M and 0.04 M–0.01 M, respectively, while zinc concentration was kept constant.
- Among all compositions, the sample containing 0.14 M Cu and 0.02 M Sn doped with Zn exhibited the most favorable structural and optical properties.

Structural Characteristics

- X-ray diffraction confirmed the formation of crystalline CZT nanoparticles for all compositions.
- The crystallite size ranged from 8.75 nm to 53.48 nm, with the smallest size observed for the CZT2 sample and the largest for the CZT4 sample.

Effect of Copper Concentration

- An increase in copper molar concentration in the host lattice was found to promote crystallite growth beyond a certain level.

Defect Analysis

- Dislocation density was observed to be inversely proportional to crystallite size, with higher defect density occurring in samples with smaller crystallites (on the order of 10^{-2} nm^{-2}).

Optical Properties

- UV–visible analysis revealed a band gap of approximately 4.4 eV, indicating strong dependence of optical properties on precursor composition.

Elemental Composition

- EDAX analysis confirmed the presence of Cu, Zn, and Sn in the synthesized material without detectable impurities.

Raman Spectroscopic Validation

- Raman spectroscopy showed characteristic CZT peaks at 262, 287, 302, 338, 367, and 374 cm^{-1}, confirming phase formation and structural integrity.

Gas Sensing Performance

- Preliminary NO_2 gas sensing studies demonstrated a saturation response time of approximately 85 s for the sample with a 3.8 eV band gap, indicating potential sensing applicability.

REFERENCES

[1] Single-phase, high-purity Cu2ZnSnS4 nanoparticles via a hydrothermal route Shih-Jen Lina, Jyh-Ming Tinga,∗, Yaw-ShyanFub,∗

[2] Influence of solvent on the properties of CZTS nanoparticles
A G Kannana, T E Manjulavallia,*, J Chandrasekaranb

[3] Facile synthesis of ultrafine Cu2ZnSnS4 nanocrystals by hydrothermal method for use in solar cells Wenchao Liu a, ∗, BingleiGuo a , CheeleungMak c, ∗, Aidong Li a , Xiaoshan Wu b , Fengming Zhang a,b

[4] A review on energy economics and the recent research and development in energy and the Cu2ZnSnS4 (CZTS) solar cells: A focus towards efficiency S.A. Khalate, R.S. Kate, R.J. Deokate∗

[5] Nanocomposite synthesis and characterization of Kesterite, Cu2ZnSnS4 (CZTS) for photovoltaic applications Elizabeth K. Michaela , Danielle Norcinib , Sridhar Komarnenic,n , Jeffrey R.S. Brownsond

[6] Simplistic toxic to non-toxic hydrothermal route to synthesize Cu2ZnSnS4 nanoparticles for solar cell applications S.A. Vanalakara,b,c,⇑ , A.S. Kamble a , S.W. Shin a , S.S. Mali d , G.L. Agawane a , V.L. Patil b , J.Y. Kim c , P.S. Patil d , J.H. Kim a,⇑

[7] One-pot hydrothermal synthesis and fabrication of kesterite Cu2ZnSn(S,Se)4 thin films Zhengqi Shi, Ahalapitiya H. Jayatissa∗

[8] Green Synthesis of Nanocrystalline Cu2ZnSnS4 Powder Using Hydrothermal RouteShrikantVerma,1 VikashAgrawal,1 KiranJain,1 RenuPasricha,2 andSureshChand1

[9] Status review and the prospects of CZTS based solar cell – A novel approach on the device structure and material modeling for CZTS based photovoltaic device M. Ravindirana,∗, C. Praveenkumarb

[10] Secondary phases and temperature effect on the synthesis and sulfurization of CZTS E. Indubalaa,c, S. Sarveshvaranb, V. Sudhac, Aamir

Y. Mamajiwalab, S. Harinipriyaa,c,∗

[11] Multifunctional CZTS thin films: Structural, optoelectrical, electrical and photovoltaic properties
S.S. Fouad, I.M. El Radaf, Pankaj Sharma, M.S. El-Bana

[12] Graded band-gap engineering for increased efficiency in CZTS solar cells H. Ferhatia , F. Djeffal a, b

[13] Solvothermal synthesis of Cu2ZnSnS4 (CZTS) nanocrystals for photovoltaic applications Bharati Patro1 , S. Vijaylakshmi1,*, Raj Kumar Reddy2 , Pratibha Sharma3

[14] Nanostructuring for enhanced absorption and carrier collection in CZTSbased solar cells: Coupled optical and electrical modeling Omar A.M. Abdelraouf, Nageh K. Allam⇑

[15] Synthesis and characterization of chemical spray pyrolysed CZTS thin films for solar cell applications
KiranDiwatea, KakasahebMohiteb, Manish Shindec, SachinRondiyaa, AmitPawbakea, Abhijit Dated, HabibPathane, SandeshJadkare,*

[16] Secondary phases and temperature effect on the synthesis and sulfurization of CZTS E. Indubalaa,c , S. Sarveshvaranb , V. Sudhac , Aamir Y. Mamajiwalab , S. Harinipriyaa,c,∗

[17] A chemical approach for synthesis of photoelectrochemically active Cu2ZnSnS4 (CZTS) thin films M.P. Suryawanshia,b , S.W. Shin a , U.V. Ghorpade a , K.V. Gurav a , G.L. Agawane a , Chang Woo Hong a , Jae Ho Yun c , P.S. Patil b , Jin Hyeok Kim a,⇑ , A.V. Moholkar b,

[18] CZTS stoichiometry effects on the band gap energy Claudia Malerbad,a,⇑ , Francesco Biccari a , Cristy Leonor Azanza Ricardo d , MatteoValentinie,a , Rosa Chierchia a , Melanie Müller d,f , AntoninoSantoni c , Emilia Esposito b , PietroMangiapane a , Paolo Scardi d , Alberto Mittiga a

[19] A review on pulsed laser deposited CZTS thin films for solar cell applications S.A. Vanalakara,b , G.L. Agawane a , S.W. Shin a , M.P. Suryawanshi a , K.V. Gurav a , K.S. Jeon a , P.S. Patil c , C.W. Jeong d , J.Y. Kim b , J.H. Kim a,⇑

[20] CZTS layers for solar cells by an electrodeposition-annealing route Md Ibrahim Khalil, Roberto Bernasconi, Luca Magagnin.